



Corneal surface area: an index of anterior segment growth

Richard A. Stone¹, Ton Lin¹, Reiko Sugimoto¹, Cheryl Capehart¹,
Maureen G. Maguire¹ and Gregor F. Schmid²

¹Department of Ophthalmology, Scheie Eye Institute, D-603 Richards Building, University of Pennsylvania School of Medicine, Philadelphia, PA 19104-6075, USA and ²Institut de Recherches en Ophthalmologie, Sion, Switzerland

Summary

Corneal surface area and perimeter were assessed as novel indices to monitor anterior segment growth, using chicks reared under different photoperiods. We obtained central and mid-peripheral corneal curvatures using photokeratometry. Anatomical tracings of the anterior corneal surface also were made from freeze-dried non-fixed preparations of the anterior segments of the same eyes. Using either photokeratometry or anatomical data, the profile of the anterior corneal surface was fit to a general equation for conical sections; corneal surface area was estimated from surfaces of revolution. Optical techniques modeled the chick cornea as a circle or as an ellipse closely resembling a circle. The anatomical technique, in contrast, modeled the chick corneal profile as a hyperbola. Potential explanations of this discrepancy are discussed. Regardless of which model is evaluated, the corneal surface area and perimeter of two-week-old chicks are affected by the photoperiod of rearing. Corneal surface area in particular proved more sensitive than conventional measurements in identifying anterior segment effects of rearing under different photoperiods. Analysis of corneal area may prove useful in evaluating the mechanisms governing anterior segment growth. © 2001 The College of Optometrists. Published by Elsevier Science Ltd. All rights reserved.

Introduction

Despite a vast clinical literature and an expanding experimental literature, the mechanisms that guide post-natal eye growth toward emmetropia or underlie the development of refractive errors remain ill-defined (Troilo, 1992). Among the ocular components, vitreous chamber depth, lens power and corneal curvature are the most important determinants of refractive state (Sorsby *et al.*, 1957; Scott and Grosvenor, 1993). How other features of the anterior segment might relate to refractive development is less well-understood (Goss and Erickson, 1987; Koretz *et al.*, 1995; Carney *et al.*, 1997; Horner *et al.*, 2000).

Post-natal eye development is commonly studied in chicks, not only because of the rapid growth and high optical quality of their eyes but also because numerous experimental protocols predictably alter ocular growth, form and refraction. In experimental animals such as chick but also in children, research on the role of the anterior segment in refractive development generally relies on keratometric assessments of central corneal curvature and ultrasound measurements of central anterior chamber depth and lens thickness. Importantly, a dissociation of the mechanisms controlling anterior segment and vitreous chamber growth has been noted many times in chicks. As examples, constant light rearing shallows the anterior chamber but lengthens the vitreous chamber (Li *et al.*, 1995; Stone *et al.*, 1995); and local administration of toxins to specific sub-types of retinal neurons can selectively affect anterior chamber or vitreous chamber growth, depending on the individual agent (Wildsoet and Pettigrew, 1988; Ehrlich *et al.*, 1990).

While defining refractive properties, the conventional ocular parameters of anterior chamber depth and corneal

Received: 17 January 2000
Revised form: 22 November 2000
Accepted: 26 November 2000

Correspondence and reprint requests to: Dr Richard A. Stone. Tel.: +1-215-898-6950; fax: +1-215-898-0528.
E-mail address: stone2@mail.med.upenn.edu (R. A. Stone).

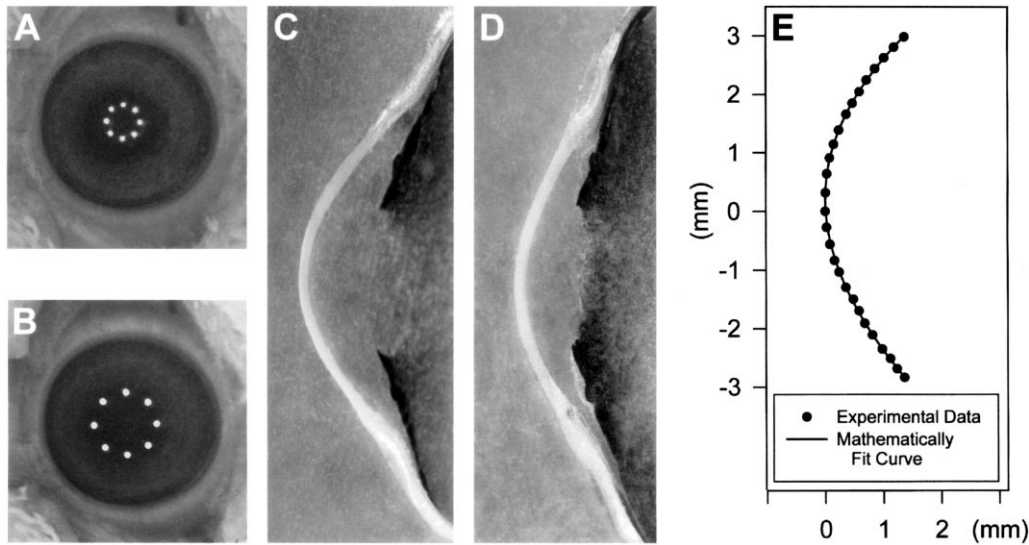


Figure 1. Photokeratometry and anatomical representations. The relative position of the first Purkinje image reflected from the anterior corneal surface is illustrated at 1:2 magnification (A) and at 1:1 magnification (B) for a chick reared under a 12 h light:dark cycle. The block face of paraffin embedded freeze dried anterior segments consistently provided clear images of the corneal contour without evident distortions. The corneal curvature from a chick reared in a 12 h light:dark cycle (C) is visibly steeper than that from a chick reared under constant light (D). (E) As illustrated here for a chick reared under a 12 h light:dark cycle, the data points (● small circles) obtained from tracing the anterior corneal surface of photographs of tissue blocks of freeze dried specimens were well described by the curve (— solid line) for the generalized equation for conical sections (Eq. (1)); the calculated parameters for this specific cornea were $r_0 = 3.00$ mm and $p = -0.14$, the latter negative value characterizing the shape as a hyperbola.

curvature do not provide a direct measure of the expansion of any actual biological tissue during development and likely conform only secondarily to more fundamental structural features of the cornea and/or anterior segment. The present study addressed whether corneal surface area or perimeter might be informative regarding developmental changes in the anterior segment. We studied the cornea of newly hatched chicks reared under photoperiods already known to influence anterior chamber depth and corneal curvature (Li *et al.*, 1995; Stone *et al.*, 1995) and found that surface area can be a more sensitive index than conventional means for assessing the cornea.

Material and methods

Newborn pre-sexed White Leghorn chicks (Truslow Farms, Chestertown, MD) were housed in previously described enclosures that allowed for photoperiod control (Stone *et al.*, 1995). Illumination consisted of cool white fluorescent lights delivering an irradiance of $1.1\text{--}1.4 \times 10^{-4}$ W/cm² at chick eye level. Groups of eight–12 male or female chicks were reared under one of three different photoperiods: 4:20 h light:dark, 12:12 h light:dark or 24 h constant light. The chicks received Purina Lab Mills™ Start&Grow food and water ad lib. The chicks were anesthetized with an intramuscular mixture of ketamine (20 mg/kg) and xylazine (5 mg/kg) for all examina-

tions. The experiments conformed with the ARVO Statement for the Use of Animals in Ophthalmic and Vision Research.

At two and a half weeks of age, corneal radii of curvature and diameters were recorded photographically with a photokeratoscope similar to one previously described (Howland and Sayles, 1985). Our instrument consisted of a Contax RTS II 35 mm camera with a Zeiss S-Planar 60 mm F2.8 macro lens. A specially constructed plastic collar secured eight equally spaced jacketed 1 mm optical grade fiber strands (Edmund Scientific, Barrington, NH) around the circumference of the lens; the fibers in turn were connected to a light source. The first Purkinje image was aligned concentric with the pupil for the on-axis measurements. Photographs were obtained with the lens adjusted to either 1:2 or 1:1 magnification (*Figure 1*) and were calibrated for each magnification with metal balls of known diameter for curvatures and with a metal ruler for linear dimensions.

After corneal photography, the eyes were refracted with a Hartinger type coincidence refractometer (Aus Jena, model 110), as described by Stone *et al.* (1995); refractions are reported as spherical equivalent (spherical power + cylinder power/2). Axial length and intraocular distances were obtained with a Sonomed A-100 ophthalmic A-scan ultrasound system (10 MHz transducer; Sonomed Technology, Inc., Lake Success, NY, USA), as described (Stone *et al.*, 1995). While still under anesthesia, the chicks were

decapitated; and the axial lengths and equatorial diameters of the enucleated eyes were measured by digital calipers.

To characterize the corneal surface with an anatomical technique, the same enucleated eyes were snap frozen immediately after the caliper measurements by immersion into isopentane cooled to the temperature of liquid nitrogen. The frozen eyes were freeze dried for 5 days, and the anterior segments were isolated by dissection and embedded in paraffin. The individual eyes were sectioned parallel to the optic axis as precisely as possible until the pupil was bisected. In each experimental group, both eyes of half of the chicks were sectioned vertically, and both eyes of the rest were sectioned horizontally. The faces of the resulting tissue blocks were then photographed at $1.2\times$ power under a dissecting microscope. This method proved superior to other anatomical approaches tried in pilot experiments, avoiding fixation-related shrinkage or corneal warping and eliminating melting problems encountered with frozen sections and frozen tissue blocks.

In independent experiments to evaluate the contour of the corneal surface in the periphery, other chicks of both sexes were reared under 12 h light:dark ($n = 10$) or 24 h constant light ($n = 12$) for 2 weeks. Under general anesthesia, they were placed in a positioning device that permitted rotation along three orthogonal axes centered at the pupil. Adapting a clinical protocol that used offset fixation points on human subjects (Mandell *et al.*, 1998), the chicks were rotated in this device while maintaining the axis of the photokeratometer perpendicular to the corneal surface. With the photokeratometer lens set at 1:2 magnification, radii of curvature were obtained at the corneal center and at off-axis positions along both the nasal and temporal horizontal meridians until the limbus was reached in each direction; these data were analyzed as the mean of the curvatures from the vertical and horizontal reflections on each Purkinje image (see *Figure 1*). Based on the angular position of the chick, measurements were made every 10° through 30° and every 5° for more peripheral locations. For perspective, centering the reflected image at the location of the Purkinje reflections in the 'mid-peripheral' photokeratometry image (*Figure 1B*) corresponded to approximately 25° of rotation.

Corneal surface area calculations

In modeling the corneal surface to calculate its surface area, we used both optical and anatomical methods on the same eyes. For each approach, the profile of the anterior corneal surface was evaluated according to the following generalized equation for conical sections (Bennett, 1968; Guillon *et al.*, 1986; Carney *et al.*, 1997):

$$y^2 = 2r_0x - px^2 \quad (1)$$

where r_0 is the apical radius of curvature and p is a shape factor that relates to eccentricity and provides an index of peripheral flattening. The geometric figure described by this

equation varies as follows with the value for p : $p > 1$ for an ellipse that steepens peripherally; $p = 1$ for a circle; $0 < p < 1$ for an ellipse that flattens peripherally; $p = 0$ for a parabola; $p < 0$ for a hyperbola.

The corneal surface area was calculated as a surface of revolution (S) between $x = 0$ and $x = h$ for the curve in Eq. (2), using the standard formula (Middlemiss, 1940):

$$S = 2\pi \int_0^h y ds \quad (2)$$

where h = corneal height at its apex, and $ds = \sqrt{dx^2 + dy^2}$.

The value for h was obtained directly from the measured diameter d of the cornea using Eq. (1), since the point at $x = h$ and $y = d/2$ is a point on the cornea. All corneal diameter measurements were obtained from the photographs because the location of the corneal edge was less ambiguous photographically than on the tissue blocks (*Figure 1*).

Substituting Eq. (1) into Eq. (2), with simplification, yields

$$S = 2\pi \int_0^h \sqrt{x^2 p(p-1) + 2r_0 x(1-p) + r_0^2} dx. \quad (3)$$

The computation of Eq. (3) was performed using trapezoidal numerical integration (Anton, 1980) at a uniform spacing of $h/100$ and Matlab software (Hanselmann and Littlefield, 1995).

To estimate r_0 and p for Eq. (3) by photokeratometry, the central corneal radius of curvature, r_0 , was obtained directly as the radius measurement in the 1:2 magnification photographs (*Figure 1A*), the magnification that yielded the smallest corneal image with conveniently measured reflections. A mid-peripheral corneal radius of curvature, r_{mp} , was obtained from the corneal reflection in the 1:1 magnification photographs (*Figure 1B*). The value x_{mp} , defined as the distance from the optical axis of the reflection used to establish r_{mp} , was calculated as half the distance between the two opposing image spots in the picture used to establish r_{mp} . To facilitate comparison with the anatomic modeling, the image spots on the photographs used for radii calculations and the diameter measurements had the identical orientation as the face of the tissue block for each eye.

Two separate methods were used to calculate the shape factor p from photokeratometry data (Roberts, 1994a,b). Both used an equation with the parameter e , the eccentricity of a conical section, where $p = 1 - e^2$. The first used a general relation of instantaneous radius of curvature as a function of apical radius of curvature, eccentricity and distance from the central axis:

$$r_{mp} = \frac{(r_0^2 + e^2 x_{mp}^2)^{3/2}}{r_0^2}. \quad (4)$$

The second used an equation for the special case where r_{mp} represents the distance between the curve and the axis along

Corneal Curvature

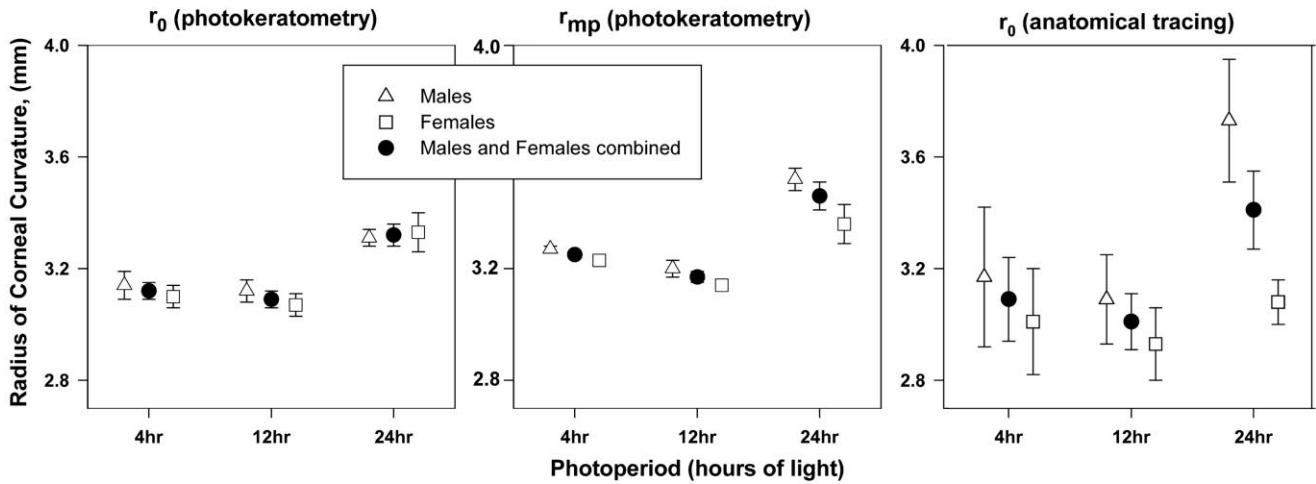


Figure 2. Photoperiod dependency of the radius of corneal curvature. The optically and anatomically derived central (r_0) and mid-peripheral (r_{mp}) radii of cornea curvature are shown for each photoperiod. The photokeratometry values were calibrated direct readings from photokeratoscope reflections at the two different positions on the corneal surface (Figure 1). The ‘anatomical tracing’ method provided r_0 from curve-fitting the contour of the anterior corneal surface on tissue blocks of freeze dried anterior segment specimens (Figure 1).

a normal to the curve at point x_{mp} (Roberts, 1994a,b):

$$r_{mp} = \sqrt{r_0^2 + e^2 x_{mp}^2} \tag{5}$$

While this latter simpler relation most properly applies only to spherical surfaces, this curvature definition underlies the output of a number of clinical corneal topography instruments (Roberts, 1994b).

To obtain corneal area with the anatomical technique, the profile of the anterior corneal surface on the face of the tissue block (Figure 1) was traced from the photographs with a digitizer pad. The data were imported into SigmaPlot (Jandel Scientific Software, San Rafael, CA), placing the corneal apex at (0, 0), and fit by non-linear regression to the curve of Eq. (1) by varying the parameters p and r_0 . To optimize the curve fit, two further transformations were used: one tilting the curve around (0, 0) and the other translating the curve laterally. The Marquardt–Levenberg nonlinear regression algorithm then was applied to determine the curve fit parameters p and r_0 that minimized the sum of the squares of the differences between the curve and the data. In using the anatomically derived values of r_0 and p to calculate surface area (Eq. (3)), the value of h was derived from the corneal diameter in the photograph oriented identically as the tissue block face.

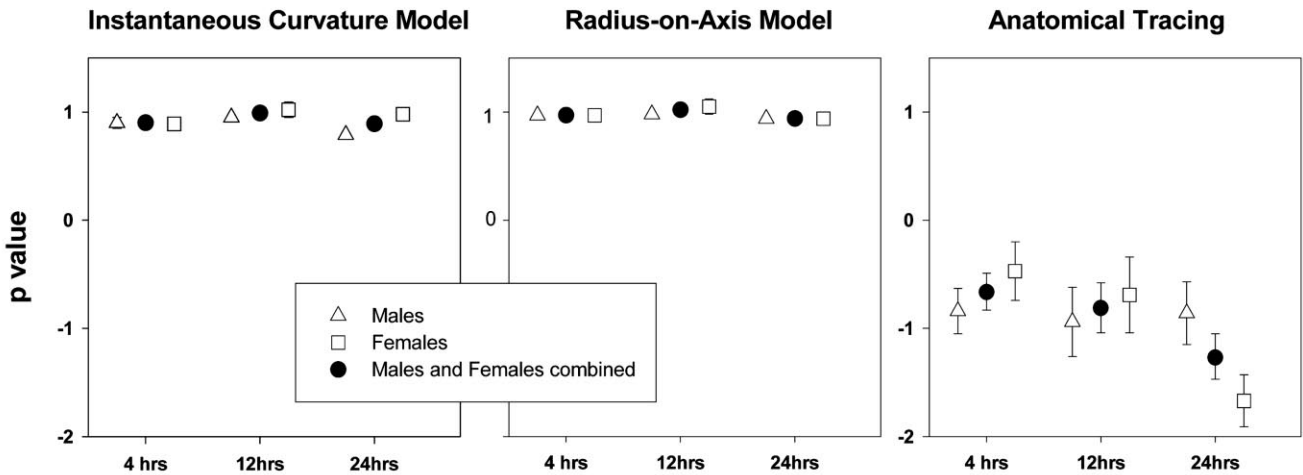
The length of the corneal perimeter was calculated from horizontal and vertical measurements of the corneal diameter obtained from the photographs used for keratometry, using the following approximate formula for the perimeter of an ellipse (Eves, 1987), where δ_h and δ_v are half the corneal diameters in the horizontal and vertical orienta-

tions respectively:

$$\text{perimeter} = 2\pi \sqrt{\frac{\delta_h^2 + \delta_v^2}{2}} \tag{6}$$

There were no systematic differences between the left and right eyes; and unless otherwise specified, the mean values for the two eyes of individual chicks were used for data analysis. Computations for statistical analyses were performed in the SAS software package (SAS Institute, 1989). SAS procedure GLM was used for the analysis of variance (ANOVA). Means \pm S.E.M. are presented in tables and graphs. Two-way ANOVA techniques evaluated whether the fixed effects of chick sex and photoperiod influenced the magnitude of refractions or eye measurements. Three-way ANOVA techniques assessed whether the fixed effects of chick sex, photoperiod or axis of diameter influenced the magnitude of the corneal diameter or corneal perimeter. Multivariate analysis techniques were used for a simultaneous analysis of the three different techniques for calculation of corneal characteristics presented in Figures 2 and 3. Again, chick sex and photoperiod were considered fixed effects and repeated measures were specified to accommodate the fact that three techniques for calculation of corneal characteristics were used on the same animals. For each individual ANOVA, the Tukey–Kraemer method with the error rate set at 0.05 was used to adjust for multiple comparisons (Kraemer, 1956). When comparing means, comparisons that were not associated with an alpha error level of 0.05 or less were referred to as not different or not statistically significantly different. Customized SAS macros (Lipsitz and

A) Corneal Shape Factor, p



B) Corneal Surface Area

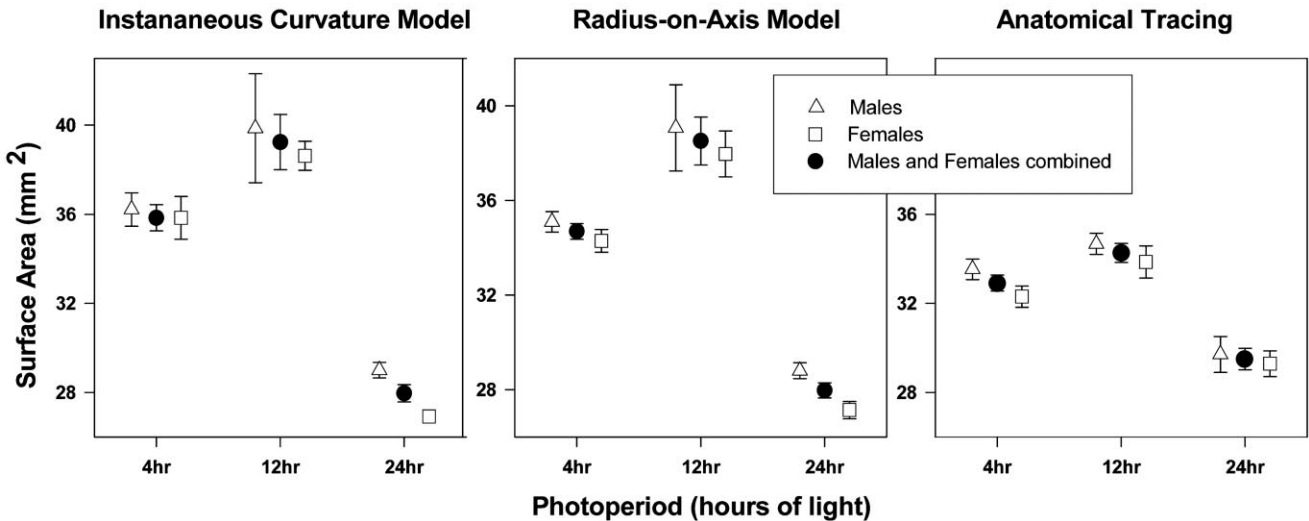


Figure 3. Photoperiod dependencies of the corneal shape factor p and the corneal area. The corneal shape factor p (Eq. (1)) and the corneal areas were each determined by three different methods. (A) For the corneal shape factor p , the ‘instantaneous curvature model’ and the ‘radius-on-axis model’ used the photokeratometry values of r_0 and r_{mp} and the calculation of the corneal shape factor p by Eq. (4) and Eq. (5), respectively. The ‘anatomical tracing’ method provided the shape factor p directly from the contour of the anterior corneal surface on tissue blocks of freeze dried anterior segment specimens. (B) The corneal surface area of chicks after 2 weeks of rearing under different photoperiods were calculated according to Eq. (3), with different determinations of r_0 and p . Areas with the ‘instantaneous curvature model’ and the ‘radius-on-axis model’ are based on photokeratometry values of r_0 and r_{mp} to calculate p according to Eq. (4) or Eq. (5), respectively. The ‘anatomical tracing’ surface areas were calculated using r_0 and p values obtained directly from the frozen tissue blocks.

Harrington, 1990) were used to apply linear regression techniques, adjusted for multiple observations per chick (Liang and Zeger, 1986), to the data on corneal surface curvatures across the horizontal meridian obtained from the surface reflections (Figure 4). Almost all comparisons in the text or figure legends used the analytical methods described above; and accordingly, comparisons identified as statistically significant indicate $P \leq 0.05$. In a few instances, Student’s t -tests

were used; and both the test and any $P \leq 0.05$ are explicitly stated in the text.

Results

Refraction and eye size

With photoperiods of either 4 or 12 h of light, the

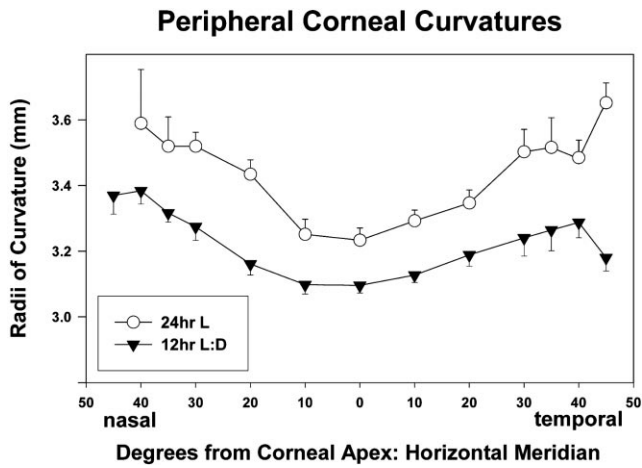


Figure 4. Corneal surface curvatures across the horizontal meridian. Corneal surface curvatures were measured across the horizontal meridian using Purkinje images obtained by off-axis orientation of the photokeratometer (see text).

ocular refractions of male and female chicks were not different; under constant light, both sexes became hyperopic but with a more pronounced response in females (Table 1). In addition to refraction, the effects of photoperiod on eye growth (data not shown) were similar to prior observations on the control open eyes of White Leghorn chicks of similar age that were reared with a unilateral lid suture but not separately analyzed by sex (Stone *et al.*, 1995). Briefly, the present results confirmed statistically that male chicks of this age have larger eyes than females by ultrasound and equatorial caliper measurements (Zhu *et al.*, 1995; Schmid and Wildsoet, 1996), but now under added photoperiods (data not shown). Rearing in constant light elongated the vitreous chamber but induced a hyperopic refractive shift because of marked corneal flattening and anterior chamber shallowing. The caliper measurements (data not shown) also confirmed that constant light rearing stimulates vitreous chamber expansion preferentially in the axial dimension (Stone *et al.*, 1995). The anterior chamber depths for chicks reared under either 4 or 12 h of light were similar to each other but deeper than those of chicks with constant light rearing (Table 2).

Corneal curvature

Photokeratometry allowed comparison of horizontal and vertical radii of curvature on individual eyes. Under most experimental conditions, the radii of curvature in the horizontal and vertical meridians were not statistically different for either the central or the mid-peripheral readings. The only consistent difference in horizontal and vertical curvatures developed under 24 h lighting and even here only for r_{mp} [horizontal/vertical r_{mp} in mm (paired *t*-tests): males = $3.45 \pm 0.03/3.49 \pm 0.03$, *P* not significant; females = $3.26 \pm 0.04/3.35 \pm 0.04$, *P* < 0.005; males and females combined = $3.36 \pm 0.03/3.42 \pm 0.03$, *P* < 0.001]. As there was otherwise no consistent trend in toricity, the effects of photoperiod and gender on corneal radii of curvature are shown as the mean of the horizontal and vertical values (Figure 2).

Because the optically and anatomically derived curvatures were obtained on the same chicks, comparing the values allows a comparison of the methods. Although the anatomical method did result in higher inter-subject variability than the optical method, there were no statistically significant differences between the optically and anatomically derived values for r_0 , and the mean values were essentially equivalent with the two techniques (Figure 2).

Overall, the larger radii of curvature of corneas of chicks reared under constant lighting were statistically different compared to those of chicks reared under the other two photoperiods (Figure 2). When considered individually, the optically derived values for r_0 and r_{mp} both were significantly flatter under constant illumination. When analyzed alone, the anatomically derived values for r_0 followed this relationship for photoperiod but did not reach statistical significance because of the high variability. There were no statistically significant differences in the central corneal curvatures comparing chicks reared under 4 or 12 h of light. From the optical measurements, the slightly larger value for r_{mp} than that of r_0 under each photoperiod did reach statistical significance given the comparatively narrow range of values under each condition. Based on the statistical analysis, both the optical determination of r_{mp} and the anatomical determination of r_0 revealed flatter corneas for males than females under constant light but not under the other photoperiods; there were no statistically

Table 1. Refractions (diopters; mean \pm S.E.M.). (The refractions after rearing under 4 or 12 h of light did not differ statistically from each other, but the refractions with constant light rearing were significantly more hyperopic. The only statistically significant sex difference occurred under constant light rearing, with females becoming more hyperopic than males.)

Photoperiod	Males	<i>n</i>	Females	<i>n</i>	Males and females combined
4 h L/20 h D	+ 0.86 \pm 0.35	8	+ 1.00 \pm 0.31	8	+ 0.93 \pm 0.23
12 h L/12 h D	+ 1.24 \pm 0.23	12	+ 1.18 \pm 0.32	10	+ 1.21 \pm 0.18
24 h L	+ 4.05 \pm 0.46	8	+ 7.71 \pm 1.51	8	+ 5.88 \pm 0.90

Table 2. Anterior segment indices (mm; mean \pm S.E.M.). (The shallower anterior chamber under constant light was statistically different from that of the other two photoperiods, which did not differ from each other; there were no gender differences in anterior chamber depth. Under each photoperiod, the slightly longer horizontal than vertical corneal diameters were statistically significant for each gender. The horizontal and vertical diameters are smaller statistically after rearing under constant light for each gender than in the other two photoperiods; but the corneal diameters after rearing under 12 or 4 h of light did not differ from each other. As with overall eye size, the corneal diameters in males were slightly greater than in females under each condition, statistically significant relationships. The corneal perimeter conformed with the diameter measurements from which they were derived. As ascertained statistically, males had longer corneal perimeters than females; and the corneal perimeters of chicks reared under constant light were shorter than those of chicks reared under the other two photoperiods, which did not differ from each other.)

	Males	Females	Males and females combined
Anterior chamber depth			
4 h L/20 h D	1.47 \pm 0.02	1.47 \pm 0.03	1.47 \pm 0.02
12 h L/12 h D	1.47 \pm 0.03	1.46 \pm 0.02	1.46 \pm 0.02
24 h L	1.11 \pm 0.02	1.03 \pm 0.03	1.07 \pm 0.02
Corneal diameter			
4 h L/20 h D			
Horizontal	5.78 \pm 0.03	5.72 \pm 0.05	5.74 \pm 0.06
Vertical	5.70 \pm 0.02	5.61 \pm 0.03	5.65 \pm 0.02
12 h L/12 h D			
Horizontal	5.82 \pm 0.03	5.78 \pm 0.05	5.80 \pm 0.03
Vertical	5.76 \pm 0.03	5.64 \pm 0.05	5.69 \pm 0.03
24 h L			
Horizontal	5.51 \pm 0.04	5.33 \pm 0.04	5.42 \pm 0.03
Vertical	5.34 \pm 0.02	5.20 \pm 0.03	5.27 \pm 0.02
Corneal perimeter			
4 h L/20 h D	17.96 \pm 0.08	17.72 \pm 0.12	17.83 \pm 0.08
12 h L/12 h D	18.16 \pm 0.13	17.77 \pm 0.15	17.95 \pm 0.12
24 h L	17.14 \pm 0.09	16.72 \pm 0.13	16.93 \pm 0.09

significant gender differences in the optically determined values of r_0 .

Corneal shape: photokeratometry analysis

Both of the two methods of calculating the corneal shape factor p from photokeratometry data (Eqs. (4) and (5)) yielded values equal to or slightly below one for each photoperiod (*Figure 3A*); presumably because of the small variability, slight differences between the two models did reach statistical significance. Because each photokeratometry method provided values for the corneal shape factor p that equaled or were slightly below one, the optical analysis suggested a sphere or an almost spherical ellipsoid as the shape for the chick cornea. There was no photoperiod effect on the shape factor p demonstrated by the radius-on-axis modeling; with the small variability, the instantaneous curvature model did yield an only slightly lower but statistically different p value under 24 h than under 12 h of light. There were no statistically significant gender effects on p .

Corneal shape: anatomical analysis

The corneal shape appeared well preserved with the histologic processing used here (*Figure 1C and D*), aided perhaps by structural support from the scleral ossicles just posterior to the limbus in the chick eye (Coulombre *et al.*, 1962). The

digitized images of the block face consistently generated curves that provided an excellent fit to the corneal contour as traced from the tissue blocks (*Figure 1E*). As there were no consistent differences between the modeling results from tissue blocks cut in either horizontal or vertical orientation (data not shown), the data were pooled from all chicks in each experimental series.

The corneal shape factor p calculated from the anatomical tracings was negative under each photoperiod (*Figure 3A*), consistent with a hyperbolic shape for the chick cornea. There were no statistically significant differences in the shape factor p between photoperiods or gender. Because the photokeratometry image for r_{mp} was in the mid-peripheral region (*Figure 1B*), we also calculated p values from the digitized anatomical profiles for each eye using only the middle portion of the cornea corresponding to the region encompassed by these mid-peripheral images. Even with analysis of the digitized profiles restricted to this middle corneal region, the corneal shape factor p for most eyes remained negative (data not shown), thus excluding abrupt flattening of the chick cornea in its far periphery as a simple explanation for the hyperbolic modeling by the anatomical method.

Corneal shape: off-axis optical measurements of peripheral surface contour

To explore further the peripheral corneal contour, we

surveyed surface curvatures away from the optic axis in both directions along the horizontal meridian by modifying a procedure used to obtain a topographical profile of the peripheral human cornea (Mandell *et al.*, 1998); the data were analyzed by linear regression. The curve for chicks reared under a 24 h photoperiod was above that of chicks reared under a 12:12 h light:dark period (Figure 4; $P < 0.001$), confirming flatter corneas in the birds reared under constant light. Because of the difficulty of obtaining complete image reflections in the far corneal periphery from some chicks, the analysis of the peripheral curvatures was restricted to curvatures at the 30–40° positions in each direction to insure a complete data set. On this basis, the cornea was steeper peripherally than centrally for chicks reared under either the 12:12 h light:dark period or constant light ($P < 0.0001$, for each curve). There were no statistically significant differences in comparing the curvatures in the nasal to temporal periphery for chicks reared under either condition.

These *in vivo* off-axis curvature measurements of the corneal surface measured a greater degree of peripheral flattening (Figure 4) than revealed by Purkinje image measurements in the mid-periphery (Figure 3A). Specifically for corneas of chicks reared under 12:12 h light:dark, the modified off-axis optical method (Figure 4) yielded a mean difference of 0.16 ± 0.03 mm between the curvatures at the corneal apex and the 30° eccentricity, compared to a mean difference of 0.07 ± 0.02 mm ($P < 0.05$, unpaired *t*-test) for the difference between r_0 and r_{mp} under the same conditions (Figure 2). Similarly for corneas of chicks reared under constant light, the mean difference between the curvatures at the corneal apex and the 30° eccentricity was 0.25 ± 0.01 mm by the off-axis optical method (Figure 4), compared to a mean difference of 0.14 ± 0.03 mm ($P < 0.05$, unpaired *t*-test) for the difference between r_0 and r_{mp} under the same condition (Figure 2).

Corneal diameter and perimeter

The corneal diameter measurements did not differ significantly in comparing readings from photographs at either magnification. Data only at the lower magnification are shown (Table 2) and used for calculations, as perhaps the greater depth of field at the lower magnification provided more accuracy. There were no statistically significant differences in corneal diameter or perimeter comparing photoperiods of 12 or 4 h of light, but both diameter and perimeter were reduced after constant light rearing.

Corneal surface area calculations

The three methods used to calculate corneal surface area differed in the values of r_0 and the shape factor p that were substituted into Eq. (3) to generate surface areas (Figure 3B). Using photokeratometry values of r_0 and r_{mp} to calcu-

late the shape factor p , the ‘instantaneous curvature model’ and the ‘radius-to-axis model’ are the areas with p obtained from Eqs. (4) or (5), respectively. The ‘anatomical tracing’ surface areas used the values obtained directly from curve-fitting the digitized corneal contour on tissue blocks. Each method for modeling corneal surface area revealed a marked and similar pattern of photoperiod dependency (Figure 3B). With each method, the corneal surface area was significantly smaller after rearing under constant light than under the other two photoperiods. For the two optical models of the corneal surface, all three photoperiods resulted in corneal surface areas that were statistically different from each other. Also for the anatomical method, the surface areas after rearing under 4 and 12 h of light were statistically different from each other. There were no significant differences in corneal surface areas comparing male to female chicks.

Discussion

Corneal shape

For optical analysis, investigators have long modeled the corneal surface as a conical section (Guillon *et al.*, 1986; Fowler and Dave, 1994). Two of the present results further validate the use of a conical section to model the corneal surface. In the anatomical analysis, Eq. (1) consistently provided an excellent mathematical fit for the digitized profile of the anterior corneal surface on tissue blocks (Figure 1E). Also, the off-axis optical assessments of peripheral surface contour (Figure 4) revealed a horizontal symmetry at the corneal apex, as the rate of flattening was similar in the nasal and temporal directions.

The approaches used here, however, provide distinctly different geometric shapes for the profile of the anterior surface of the chick cornea, specifically in the pattern of peripheral flattening (Figure 3A). Using Purkinje images at two locations and either of two equations previously applied to the human cornea (Eqs. (4) or (5)), modeling the corneal surface yields values of the corneal shape factor p equal to or slightly below one, implying the profile of a circle or an ellipse that is close to circular. In contrast, the anatomical method consistently yields negative numerical values for the shape factor p , implying a hyperbolic profile.

The shape discrepancies are not readily resolved since potential artifacts can arise either from inherent uncertainties in using two-dimensional photokeratometry images from surface reflections of the peripheral cornea to reconstruct the three-dimensional corneal shape (Wilson *et al.*, 1992; Roberts, 1994a,b) or from tissue effects of the anatomical processing. Sampling bias seems excluded: the anatomical tracing was made post-mortem on the identical corneas from which photokeratometry was performed *in vivo*; and for each individual eye, curvature and diameter measurements from the identical meridian were incorporated into

the calculations regardless of method. Restricting the anatomical analysis to the corneal region encompassed by the mid-peripheral Purkinje images also did not reconcile the corneal shape factor p with the values calculated from optical measurements. The discrepancy cannot clearly be ascribed to potential artifacts of anatomical processing either: the mean values of the central corneal curvatures (r_0 ; *Figure 2*) as calculated from the digitized anatomical profiles, despite their higher variability, corresponded well with the curvatures measured from photokeratometry images in the central corneal region where optical methods are least ambiguous (Wilson *et al.*, 1992). The off-axis corneal curvature measurements (*Figure 4*) by optical methods provide an independent method suggesting that the use of Purkinje images in the periphery underestimates the degree of corneal flattening in the periphery, at least with spherically-based calibrations as also commonly assumed for clinical topography (Roberts, 1994b). These results thus suggest that, compared the optical modeling using conventional approaches to on-axis Purkinje images, the present anatomical modeling may be more suited for determining the area of the chick cornea.

The implication of this discrepancy in chicks for modeling the shape of the human cornea is unclear. Clinical corneal topography instruments typically model corneal contours from the first Purkinje image, as a Placido disc, and require simplifying assumptions to model the peripheral corneal surface (Wilson *et al.*, 1992; Roberts, 1994b); even when used to describe corneal contour as distinct from corneal power, these instruments require simplifying approximations and may induce significant error (American Academy of Ophthalmology, 1999). While the shape factor p for the human cornea shows considerable individual variability when modeled with Purkinje images, it generally falls in the 0–1 range with a peak value near $p = 0.8$; rarely, $p > 1$ is obtained (Guillon *et al.*, 1986; Bennett and Rabbetts, 1991). Use of analogous optical methods for the chick cornea generated p values in the range commonly measured for humans. A recent videokeratographic study of the human cornea with offset fixation revealed a greater rate of peripheral flattening than previously detected by conventional topography (Mandell *et al.*, 1998); together with the present findings in the chick, these results underscore the difficulties in modeling the peripheral human cornea from Purkinje images.

Corneal surface area

Despite the ambiguities in corneal surface modeling, each approach indicated that corneal surface area can be more sensitive in assessing development than the conventional anterior segment measurements of corneal curvature, corneal diameter or anterior chamber depth. Recent clinical reports have suggested that the corneal shape factor is potentially useful in studying refractive development (Carney *et al.*, 1997; Horner *et al.*, 2000); but at least in

chick, area may be even more sensitive than shape in revealing subtle anterior segment changes since only area measurements identified a difference between rearing under 4 and 12 h of daily light (*Figure 3*). An effect of photoperiod on the cornea has been detected many times previously in neonatal chicks (Li *et al.*, 1995; Stone *et al.*, 1995); but only in terms of the pronounced effects of constant light rearing and not the more subtle differences revealed here. Further, area measurements directly indicate that photoperiod alters corneal size rather than simply influencing its form and suggest that the changes in curvature followed definable effects on corneal growth.

Since the corneal surface area calculation (Eq. (3)) utilizes the corneal shape factor p , differences in surface area between calculations based on the optical and anatomical measurements are to be expected (*Figure 3B*). In this instance, anatomical measurements provided smaller estimates for surface areas than optical measurements for rearing under 4 or 12 h of light, but comparable areas for the constant light rearing where the overall corneal profile is flattest.

The conventional measurements of corneal curvature and anterior segment depth should depend geometrically on the corneal surface area and perimeter. Alterations in the surface area and/or perimeter could account for any experimental influence on corneal curvature or anterior chamber depth. The differences in corneal surface area between rearing in 4 or 12 h of light (*Figure 3B*) indicate that alterations in corneal expansion may occur without evident effects on the conventional measures of central corneal curvature or diameter. Thus, corneal surface area might prove useful in identifying mechanisms governing anterior segment growth and reveal more active developmental mechanisms in the cornea than presently appreciated (Mutti *et al.*, 1998).

Acknowledgements

This research was supported by National Eye Institute grants R01 EY07354 (R.A.S.) and R21 EY10964 (M.G.M.), by an unrestricted gift to the Department of Ophthalmology, University of Pennsylvania, from Research to Prevent Blindness, and by the Paul and Evanina Bell Mackall Foundation Trust.

References

- American Academy of Ophthalmology (1999). Corneal topography. *Ophthalmology* **106**, 1628–1638.
- Anton, H. (1980). Techniques of integration. In: *Calculus*, John Wiley and Sons, New York, p. 528.
- Bennett, A. G. (1968). Aspherical contact lens surfaces. *The Ophthalmic Optician* **8**, 1037–1040.
- Bennett, A. G. and Rabbetts, R. B. (1991). What radius does the conventional keratometer measure? *Ophthalm. Physiol. Opt.* **11**, 239–247.
- Carney, L. G., Mainstone, J. C. and Henderson, B. A. (1997).

- Corneal topography and myopia. A cross-sectional study. *Invest. Ophthalmol. Vis. Sci.* **38**, 311–320.
- Coulombre, A. J., Coulombre, J. L. and Mehta, H. (1962). The skeleton of the eye. I. Conjunctival papillae and scleral ossicles. *Dev. Biol.* **5**, 382–401.
- Ehrlich, D., Sattayasai, J., Zappia, J. and Barrington, M. (1990). Effects of selective neurotoxins on eye growth in the young chick. In: *Myopia and the Control of Eye Growth* (eds G. Bock and K. Widdows), Ciba Foundation Symposium 155, Wiley, Chichester, pp. 63–88.
- Eves, H. (1987). Geometry. In: *CRC Handbook of Mathematical Sciences* (ed W. H. Beyer), 6th ed., CRC Press, Inc, Boca Raton, pp. 152–164.
- Fowler, C. W. and Dave, T. N. (1994). Review of past and present techniques of measuring corneal topography. *Ophthalm. Physiol. Opt.* **14**, 49–58.
- Goss, D. A. and Erickson, P. (1987). Meridional corneal components of myopia progression in young adults and children. *Am. J. Optom. Physiol. Optics* **64**, 475–481.
- Guillon, M., Lydon, D. P. M. and Wilson, C. (1986). Corneal topography: a clinical model. *Ophthalm. Physiol. Opt.* **6**, 47–56.
- Hanselmann, D. and Littlefield, B. (1995). Integration. In: *The Math Works, Inc. The Student Edition of Matlab®*, Version 4 *User's Guide*. Prentice Hall, Englewood Cliffs, NJ, pp. 135–137.
- Horner, D. G., Soni, S., Vyas, N. and Himebaugh, N. L. (2000). Longitudinal changes in corneal asphericity in myopia. *Optom. Vis. Sci.* **77**, 198–203.
- Howland, H. C. and Sayles, N. (1985). Photokeratometric and photorefractive measurements of astigmatism in infants and young children. *Vision Res.* **25**, 73–81.
- Koretz, J. F., Rogot, A. and Kaufman, P. L. (1995). Physiological strategies for emmetropia. *Trans. Am. Ophthalmol. Soc.* **93**, 105–118.
- Kraemer, C. Y. (1956). Extension of multiple range tests to group means with unequal numbers of replications. *Biometrics* **12**, 307–310.
- Li, T., Troilo, D., Glasser, A. and Howland, H. C. (1995). Constant light produces severe corneal flattening and hyperopia in chickens. *Vision Res.* **35**, 1203–1209.
- Liang, K. Y. and Zeger, S. L. (1986). Longitudinal data analysis using generalized linear models. *Biometrika* **73**, 13–22.
- Lipsitz, S. L. and Harrington, D. P. (1990). Analyzing correlated binary data using SAS. *Computers and Biomedical Res.* **23**, 268–282.
- Mandell, R. B., Corzine, J. C. and Klein, S. A. (1998). Peripheral corneal topography and the limbus. *Invest. Ophthalmol. Vis. Sci.* **39**, (Suppl.), 1036 (Abstract).
- Middlemiss, R. R. (1940). Areas of surfaces of revolution. In: *Differential and Integral Calculus*, 1st ed, McGraw-Hill Book Company, Inc., New York, pp. 219–222.
- Mutti, D. O., Zadnik, K., Fusaro, R. E., Friedman, N. E., Sholtz, R. I. and Adams, A. J. (1998). Optical and structural development of the crystalline lens in childhood. *Invest. Ophthalmol. Vis. Sci.* **39**, 120–133.
- Roberts, C. (1994a). Characterization of the inherent error in a spherically-biased corneal topography system in mapping a radially aspheric surface. *J. Refrac. Corneal Surg.* **10**, 103–111.
- Roberts, C. (1994b). The accuracy of 'power' maps to display curvature data in corneal topography systems. *Invest. Ophthalmol. Vis. Sci.* **35**, 3525–3532.
- SAS Institute Inc. (1989). *SAS/STAT User's Guide, Version 6*, Volume 2. 4th ed, SAS Institute Inc, Cary, NC.
- Schmid, K. and Wildsoet, C. (1996). Breed- and gender-dependent differences in eye growth and form deprivation responses in chick. *J. Comp. Physiol. A* **178**, 551–561.
- Scott, R. and Grosvenor, T. (1993). Structural model for emmetropic and myopic eyes. *Ophthalm. Physiol. Optics* **13**, 41–47.
- Sorsby, A., Benjamin, B., Davey, J. B., Sheridan, M. and Tanner, J. M. (1957). *Emmetropia and its Aberrations. A Study in the Optical Components of the Eye*. Medical Research Council Special Report Series, No. 293. Her Majesty's Stationery Office, London, pp. 1–48.
- Stone, R. A., Lin, T., Desai, D. and Capehart, C. (1995). Photoperiod, early post-natal eye growth, and visual deprivation. *Vision Res.* **35**, 1195–1202.
- Troilo, D. (1992). Neonatal eye growth and emmetropization—a literature review. *Eye* **6**, 154–160.
- Wildsoet, C. F. and Pettigrew, J. D. (1988). Kainic acid-induced eye enlargement in chickens: differential effects on anterior and posterior segments. *Invest. Ophthalmol. Vis. Sci.* **29**, 311–319.
- Wilson, S. E., Wang, J. -Y. and Klyce, S. D. (1992). Quantification and mathematical analysis of photokeratographic images. In: *Corneal Topography. Measuring and Modifying the Cornea* (eds D. J. Schanzlin and J. B. Robin), Springer-Verlag, New York, pp. 1–9.
- Zhu, X., Lin, T., Stone, R. A. and Laties, A. M. (1995). Sex differences in chick eye growth and experimental myopia. *Exp. Eye Res.* **61**, 173–179.